Fractal versus quasiclassical diffusive transport in a class of quantum systems

Fausto Borgonovi
Dipartimento di Matematica, Università Cattolica, sede di Brescia, via Trieste 17, 25121 Brescia, Italy
Istituto Nazionale di Fisica Nucleare, Sezione di Pavia, via Bassi 6, 27100 Pavia, Italy

Italo Guarneri
Università di Milano, sede di Como, via Lucini 3, 22100 Como, Italy
and Istituto Nazionale di Fisica Nucleare, Sezione di Pavia, via Bassi 6, 27100 Pavia, Italy
(Received 24 January 1995)

We compare the properties of transmission across one-dimensional finite samples which are associated with two types of quantum diffusion, one related to a classical chaotic dynamics, the other to a multifractal energy spectrum. We numerically investigate models exhibiting one or both of these features, and we find in all cases an inverse power-law dependence of the average transmission on the sample length. Although in all the considered cases the quadratic spread of wave packets increases linearly (or very close to linearly) in time for both types of dynamics, a proper Ohmic dependence is always observed only in the case of quasiclassical diffusion. The analysis of the statistics of transmission fluctuations in the case of a fractal spectrum exposes some new features, which mark further differences from ordinary diffusion, and enforce the conclusion that the two types of transmission are intrinsically different.

I. INTRODUCTION

The onset of chaos in classical single-particle dynamics is often accompanied by deterministic diffusion, which is a type of stochastic motion which mimics to some extent a random walk, even in the absence of external random agents. Typical examples are the motion of a particle elastically bouncing in an array of fixed scatterers and the diffusive energy absorption occurring in nonlinear periodically driven systems. In both cases, characteristic transport properties appear that can be more or less accurately described by an equation of the Fokker-Planck type. Whether similar transport properties persist on the quantum level is an important question, which lies on the borderline between quantum chaology and solid state physics, and has received much attention on both sides. A most remarkable result in this context is that chaotic diffusion is inhibited by quantization. A classical one-dimensional (1D) diffusion is quantally reproduced only on a finite time scale, and is in the long run stopped by an interference effect very similar to Anderson localization. Equivalently, if the transmission of particles across a finite sample of a quasi-one-dimensional disordered solid is considered, then the inverse dependence on the sample length characteristic of a classical diffusive transport (Ohm's law) is quantally observed only on length scales which are small in comparison with the Anderson localization length.

It was realized that, in the quasi-one-dimensional case, an unbounded diffusive (or anomalously diffusive) spreading of wave packets is often associated with a singular continuous spectrum of the Hamiltonian (or the Floquet operator in the case of periodically driven systems). This sort of a spectrum, regarded as a mathematical curiosity a long time, appears quite frequently in incommensurate structures, such as involved, e.g., in quasicrystals and electron dynamics in crystals in magnetic fields; in such cases fractal singular spectra of zero Lebesgue measure have been found. In the light of the above findings, and insofar as the quasi-one-dimensional case is concerned, a quantum "diffusive" regime, i.e., one marked by a linear (or close to linear) increase in time of the mean square displacement, can exist either due to an underlying classical chaotic diffusion, developing on small scales in which localization effects are not yet apparent, or due to a fractal structure of the spectrum, no scale limitations being necessary in the latter case.

Prototype systems for these two situations are the kicked rotator model (KRM) and the Harper (HM) model, respectively. Each of these two models exhibits one type of quantum diffusion, but not the other; therefore, the two phenomena are in principle independent of each other. Still, the question remains whether the "fractal" unbounded diffusion may offer a quantum counterpart for the classical unbounded propagation in cases when both are present. A particular aspect of this question is what kind of transmission properties are associated with the fractal diffusion and how they match with the Ohmic transport typical of classical diffusion.

We have studied this question using the two mentioned models plus a third one, which in a sense interpolates between them. This is the kicked Harper model (KHM), which displays at once a chaotic classical limit marked by deterministic diffusion (which is missing in the HM) and a "critical" quantum regime with a multifractal quasienergy spectrum (which is missing in the KRM). We have compared the properties of quantum transmission across finite samples which are observed in

0163-1829/95/52(5)/3374(9)/$06.00

the three cases. The analogies and differences we have observed supply useful indications for answering the questions raised before. For example, according to our results, Ohm's law seems to be rather exceptional inside the class of quantum systems endowed with fractal quantum diffusion. The fingerprint of this macroscopic law would be then represented by the concurrent presence of a quasiclassical diffusion.

Other differences emerge on analyzing transmission fluctuations, and lead to the conclusion that the two types of diffusion are marked by essentially different statistical properties, and are in no apparent relation to each other.

The plan of the paper is the following: In Sec. II we review the mathematical formalism which allows for a general treatment of the kicked dynamics as a scattering process. In Sec. III we present the old (Sec. III A) and the new (Secs. III B and III C) results about the transport properties respectively in the KRM, in the KHM, and in the HM. The conclusive Sec. IV is devoted to the analysis of the transmission fluctuations.

II. DISCRETE-TIME SCATTERING PROCESSES

We are interested in one-dimensional scattering processes in which free particles impinge on a "sample" of a finite length, whereby they are either reflected or transmitted. The particle dynamics inside the sample will have a nontrivial diffusive character, both in the classical and in the quantum cases. Such a situation cannot, of course, occur in strictly one-dimensional, conservative Hamiltonian cases, but it can be realized with relative ease if one considers a discrete-time dynamics instead of a continuous-time one—an artifact which has proven extremely useful in nonlinear dynamics. We shall presently outline the general formalism needed to describe a discrete-time scattering process.

We consider the discrete time dynamics of a particle on a line, with coordinate q and momentum p. Throughout this paper we shall use dimensionless variables. The classical dynamics of the particle is described by the iteration of an area-preserving map, of the form

$$\begin{aligned} \bar{q} &= q - \frac{\partial S(p)}{\partial p}, \\ \bar{p} &= \begin{cases} p + \frac{\partial V(\bar{q})}{\partial \bar{q}} & \text{if } q_0 < \bar{q} \le q_0 + L, \\ p & \text{elsewhere,} \end{cases} \end{aligned} \tag{2.1}$$

where the generating functions S, V will have different forms, depending on the considered model. In all cases, however, the function S will be even and periodic in the momentum p, with period 2π. Outside the region $q_0 < q \le q_0 + L$ the motion is uniform at constant speed $-S'(p)$ and momentum p. Thus Eqs. (2.1) define a scattering problem, in which free particles coming from infinity impinge on the scattering region, wherein they undergo "collisions" described by the "potential" $V(q)$, until they reexit from either end. With appropriate choices of the generating functions S, V, the dynamics inside the sample will have a chaotic character, leading to fast randomization in p and to diffusion in q.

In this case, the scattering trajectories sensitively depend on various parameters, including q_0, which defines the position of the scatterer on the line; both transmission and reflection are affected in an unpredictable way by small changes of q_0, because q_0, together with the incoming momentum, defines the initial conditions for the chaotic map whose iteration defines the dynamics of the particle inside the scatterer.

For this reason, we can generate statistical ensembles by placing the scatterer at different positions; different locations of the scatterer of length L will define different statistical samples in the ensemble. This is in clear analogy with the problem of electronic transmission through disordered solids. In that case different samples correspond to different realizations of disorder.

The quantization of the dynamics (2.1) is obtained in a standard way by iterating the quantum one-step propagator

$$\hat{U} = e^{\frac{i}{\hbar}V(\hat{q})} e^{\frac{i}{\hbar}S(\hat{p})}, \tag{2.2}$$

where we have introduced the adimensional Planck constant $\hbar$, and $V(q)$ is taken $\neq 0$ only for q inside the scattering region.

Due to periodicity in p, the Bloch theorem applies, and the evolution (2.2) preserves the "quasiposition" $\hat{\alpha} = \hat{q}$. The value α of the quasiposition is a constant of the motion; therefore its value can be arbitrarily fixed. The quantum dynamics at fixed α can be studied, by using the quantization rule

$$\hat{q}_\alpha = -i\hbar \frac{\partial}{\partial p} + \alpha, \tag{2.3}$$

defined on 2π-periodic wave functions. Quantized in this way, the position assumes discrete values $n\hbar + \alpha$ (n integer); that is, the quantum motion at a given quasiposition takes place on a discrete one-dimensional lattice. We shall denote $|n\rangle$ the eigenstate corresponding to the nth site of this lattice. The quantum evolution at fixed α is given by a unitary operator $\hat{U}_\alpha$ obtained by writing $\hat{q}_\alpha$ instead of $\hat{q}$ in Eq. (2.2). Whereas $\hat{U}$ acts in the space of square-summable functions on the line, $\hat{U}_\alpha$ acts in the space of square-summable functions on the lattice.

The unitary operator $\hat{U}_\alpha$ has eigenvalues $e^{i\lambda/\hbar}$, and $\lambda (\mathrm{mod} 2\pi\hbar)$ is known as the quasienergy. The quasienergy is obviously conserved under the evolution.

The quantum scattering theory stems, as usual, from a comparison of the long-time asymptotics of the dynamics generated by (2.2) with the free dynamics generated by $\hat{U}_0 = \exp[iS(\hat{p})/\hbar]$. On mathematical grounds, $\hat{U}_\alpha$ is a finite-rank perturbation of $\hat{U}_0$. This entails the existence of the Møller wave operators $\hat{\Omega}_\mp = \lim_{t\to\pm\infty} \hat{U}^t \hat{U}_0^{-t}$ and thus ensures the well-posedness of the scattering problem. In order to find the scattering matrix it is convenient to resort to time-independent scattering theory, and to seek the scattering eigenfunctions of $\hat{U}$ corresponding to a given value λ of the quasienergy. The eigenfunctions of the free dynamics corresponding to the same quasienergy are

$$\langle n | u_0^{\lambda,j} \rangle = (2\pi)^{-1/2} e^{-inp_j/\hbar}, \tag{2.4}$$

where p_j $(j = 1, ..., N_\lambda)$ are the roots of the equation

$$S(p_j) = \lambda \pmod{2\pi\hbar}.$$

In this way for each quasienergy λ there are N_λ degenerate eigenfunctions; every one of them corresponds to an open scattering channel at the given quasienergy. The number N_λ of such channels depends on the quasienergy λ and on the specific form of the function S.

The scattering dynamics can be visualized as follows: Plane waves, eigenfunctions of $\hat{U}_0$, are scattered by the sample, thus giving rise to reflected and transmitted waves. The crucial feature of this process is that quasienergy is conserved; that is, $S(p)$ is changed by an integer multiple of $2\pi\hbar$. The construction of the $\mathcal{S}$ matrix follows standard rules of the scattering theory, via the Lippmann-Schwinger equation

$$[1 - e^{i\lambda/\hbar}\hat{G}_+(e^{-i\hat{V}/\hbar} - 1)]u_+^{\lambda,j} = u_0^{\lambda,j}, \tag{2.5}$$

relating free waves u_0 with true, distorted waves u_+. In the above formula $\hat{G}_+$ is the "free" Green function:

$$\hat{G}_+(\lambda) = \lim_{\epsilon\to 0^+}(e^{i\hat{S}/\hbar} - e^{i\lambda/\hbar+\epsilon})^{-1}. \tag{2.6}$$

By inverting the system (2.5) one obtains the distorted waves u_+ and the $\mathcal{S}$ matrix, whose elements are given by

$$\mathcal{S}_{j,k} = \delta_{j,k} - 2\pi|\nu_j|^{1/2}|\nu_k|^{1/2}\langle(e^{i\hat{V}/\hbar} - 1)u_0^{\lambda,j}|u_+^{\lambda,k}\rangle, \tag{2.7}$$

where $j, k = 1, \ldots, N_\lambda$ and $|\nu_j| = 1/|dS(p_j)/dp|$ is the density of states. Given the $\mathcal{S}$ matrix, the transmission coefficient is obtained by summing the squared moduli of the $\mathcal{S}$-matrix elements related to transmission in a given direction of propagation.

The $\mathcal{S}$ matrix is sample dependent because the explicit form of $\hat{U}_\alpha$ depends on the choice of the sample, that is, on q_0, through the values of the function $A(q) = \exp[iV(q)/\hbar]$ at $q = n\hbar+\alpha$ $(q_0 < q \le q_0+L)$. The string of these $\sim L/\hbar$ values has a more or less disordered character, depending on the choice of the function $V(q)$; in any case, for any nontrivial choice of the latter, different samples correspond to different strings, and different strings correspond to different realizations of "disorder." There is a connection between the dependence of the $\mathcal{S}$ matrix on the sample and its dependence on the quasiposition α, because changing the latter by $\hbar$ is equivalent to shifting the sample by one site along the q lattice. This suggests that the above-described process of averaging over disorder may be equivalent to averaging over all possible values of the quasiposition. This is certainly true when $2\pi/\hbar$ is an irrational number and $A(q)$ is a 2π-periodic function—a case that occupies a central position in this paper. In that case, any quantity related to scattering is also a 2π-periodic function of α, and its average over all samples at given $\alpha = \alpha_0$ coincides with the average over all the values of $\alpha = \alpha_0 + n\hbar \bmod(2\pi)$, which are obtained from α_0 by iterating the shift $\alpha \to \alpha\hbar \bmod(2\pi)$. Indeed, since this shift is ergodic for $2\pi/\hbar$ irrational, such "time averages" are independent of the starting point α_0 and coincide with "phase averages," i.e., averages over α_0.

III. TRANSPORT PROPERTIES

A. Kicked rotator

With the choice $S(p) = b\cos p$, $V(q) = \frac{\tau}{2}q^2$ the map (2.1) describing the dynamics inside the sample becomes the standard map, which has been widely studied both in its classical and in its quantum versions; the latter is associated with a well-known dynamical model, known as the KRM.

The quantum KRM is a paradigm of the quantum phenomena associated with classical chaotic diffusion, and a short review of its main properties will provide a proper frame for the following discussion. At $b\tau \gg 1$ the classical standard map is fully chaotic, and the q motion is similar to a random walk, with a diffusion coefficient $D = \beta(b)b^2/2$ where $\beta(b)$ is a known bounded function of b.[1] On length scales much bigger than b, the distribution $f(q,t)$ of a statistical ensemble of orbits is adequately described by the diffusive approximation, which assumes $f(q,t)$ to satisfy the diffusion (Fokker-Planck) equation.[1–3]

The properties of the quantum KRM (at a fixed quasiposition) crucially depend on the arithmetic nature of $\hbar$. If $\hbar$ is a rational multiple of 4π, then the evolution operator (2.2) has an absolutely continuous spectral component that produces a ballistic spread of wave packets on the q lattice. If $\hbar$ is a "good" irrational number, accumulated numerical evidence supports a pure-point spectrum, and exponential localization of wave packets on the lattice, with a localization length $\ell \sim b^2/\hbar$ (the properties of the KRM are reviewed in Ref. 4). Thus in all known cases the long-time nature of the quantum propagation is different from that of the classical motion; while the latter is diffusive, the former is either ballistic or localized. Since the correspondence principle entails that in the limit $\hbar \to 0$ the classical diffusive motion must be recovered, there must be a time scale $t_D(\hbar)$ separating the quasiclassical diffusive spread of wave packets from the purely quantum regime (ballistic or localized). It is known that $t_D \sim D/\hbar$, which is the time required to diffuse over the localization length ℓ.

The scattering problem associated with the KRM was investigated in detail in Ref. 5. In the classical case, for $b \ll L$ the diffusive approximation is valid, and the numerically computed transmission coefficient T is in excellent agreement with the theoretical value:

$$\frac{1}{T} = 2 - \frac{1}{\beta} + \frac{2b}{\pi D}L, \tag{3.1}$$

which is found by solving the diffusion equation in the sample of length L, subject to appropriate boundary conditions.[5] On comparing (3.1) with the kinetic formula $T \approx \ell_0/L$ involving the mean free path (MFP) ℓ_0, we are led to $\ell_0 \sim b$. Notice that T is a sample-independent quantity.

In the quantum case, a detailed numerical analysis was carried out for the strongly incommensurate case. For any quasienergy λ a transmission coefficient $T(\lambda)$ was computed following the procedure outlined in Sec. II.

$T(\lambda)$ is a fluctuating, i.e., sample-dependent, quantity. The main facts about the statistics of this quantity that emerge from numerical computations are the following.

(1) $\langle T(\lambda)\rangle_{q_0}$ [the average of $T(\lambda)$ over q_0] is but weakly dependent on λ, and is therefore close to the total transmission [the average of $T(\lambda)$ over λ], which is the quantum counterpart for the classical transmission (3.1). It is in fact a decreasing function of L which comes close to (3.1) in a range of lengths $\ell_0 \ll L \ll \ell$, or, equivalently, $b \ll L \ll b^2/\hbar$, which is called the "diffusive regime" (see Fig. 1).

At larger lengths, $\langle T(\lambda)\rangle_{q_0}$ exponentially decreases with L, as $\exp(-2L/\ell)$; this is the localized, or "insulator," regime.

(2) In the diffusive regime, $\mathrm{Var}(T(\lambda))$ [the variance of $T(\lambda)$] is roughly independent of length.[6]

Both (1) and (2) reproduce well-known aspects of electronic transmission through quasi-one-dimensional disordered solids; in particular, the scale independence of the magnitude of transmission fluctuations observed in the diffusive regime is the celebrated phenomenon of universal conductance fluctuations (UCF's).

B. Kicked Harper model

The KHM is obtained by choosing $S(p) = d\cos p$, $V(q) = c\cos q$. It has been widely studied by many authors[7–14] (for a review on the subject see Ref. 15). It is classically chaotic and diffusive at $d, c \gg 1$, and the statistical analysis outlined for the KRM is still valid (with appropriate modifications).

The spectral properties of the quantum KHM at a fixed quasiposition, like those of the quantum KRM, depend on the arithmetic nature of $\hbar$. If the latter is commensurate with 2π, then the spectrum is absolutely continuous, and the propagation of wave packets is ballistic; a continuous spectral component is also present for "not too incommensurate" values of $\hbar$. However, even for strongly incommensurate values of $\hbar$ the spectral properties depend in a highly nontrivial way on the value of the parameters c, d. Whereas exponential localization is still present at $d \gg c$, the motion is ballistic at $c \gg d$; a phase portrait, illustrating the type of motion in various regions of the (c, d) plane, can be found in Ref. 12. These nontrivial properties of the KHM are connected with its double periodicity (in q and in p as well),[11] a feature which the KHM shares with the HM, which is the object of the next section.

In particular, at $c = d$ the motion is always delocalized, and wave packets spread according to a law $\langle(\Delta q)^2\rangle \sim t^\gamma$. The exponent γ is close to 1, but it appears to depend on the value of $c = d$. This behavior signals the presence of a singular-continuous spectral component[16,17] and in fact a multifractal spectrum has been numerically found, with a Hausdorff dimension close to 0.5.

We have investigated the question of how this (possibly anomalous) diffusion at $c = d$ is reflected in the transmission properties of the scattering model. In our numerical computations we have used the function $2\arctan[\epsilon\cos(\cdot)]/\epsilon$ with $\epsilon << 1$ as an approximation for the function $\cos(\cdot)$ appearing in the generating functions S, V. The dependence of the classical transmission on the sample length is shown by the dashed line in Fig. 2 and by the solid one in Fig. 3; as in the KRM, it follows the law (3.1) with the appropriate parameters.

The behavior of the quantum $\langle T(\lambda)\rangle_{q_0}$ depends on whether λ is chosen in the spectrum or not. In strongly incommensurate cases, the quantum spectrum is singular, i.e., has zero Lebesgue measure, and $\langle T(\lambda)\rangle_{q_0}$ is exponentially small at large L for almost all values of the quasienergy λ. Therefore, the total transmission, too, is exponentially small at large L, at variance with the classical behavior, which follows the law (3.1) instead.

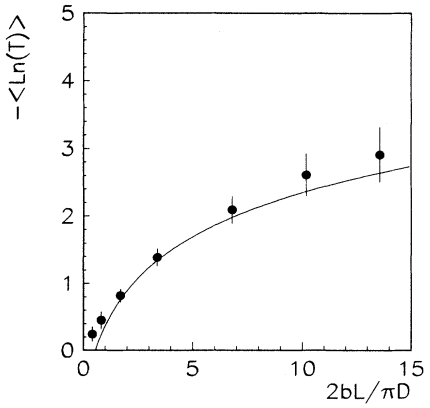

FIG. 1. Transmission versus the rescaled sample length (in units of the mean free path) for the KRM. Solid symbols are quantum data for $b\tau = 10$, $b = 58$, $\hbar = 1$. Each point is obtained by averaging over an ensemble of $10^2, 10^3$ different samples. The quasienergy λ is fixed. The solid line is the classical theoretical prediction (3.1).

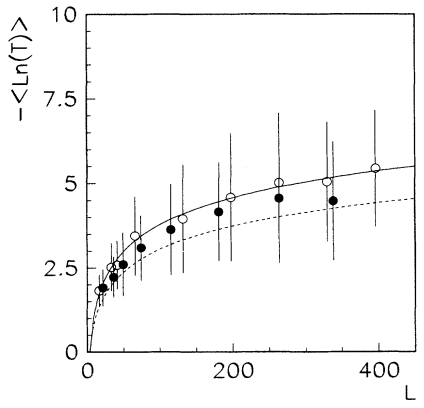

FIG. 2. Transmission versus the sample length for the KHM and $c = d = 10$, $\hbar/2\pi = 144/1097$. Solid and open circles are relative to two quasienergies in the middle of two different bands. The solid line is the best fit for open circles. Each point is obtained by averaging over an ensemble of 10^2 different samples. The dashed line is the corresponding classical line from a kinetic equation like (3.1) with the classical diffusion coefficient.

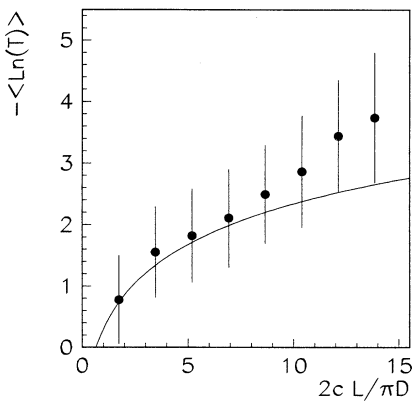

FIG. 3. Transmission versus the rescaled sample length (in units of the mean free path) for the KHM. Solid symbols are quantum data for $c = d = 10$, $\hbar = 2\pi/(6+\rho)$, ρ the golden mean. Each point is obtained by averaging over an ensemble of 500 different samples. The quasienergy λ is fixed. The solid line is the classical theoretical prediction.

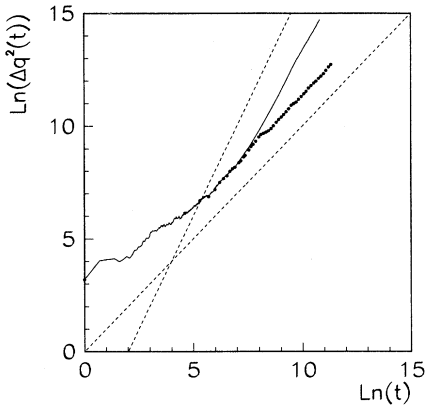

FIG. 4. Energy growth in time for the KHM, for $c = d = 10$ and rational $\hbar/2\pi$ approximant to $1/(6+\rho)$, ρ being the golden mean. The solid line is for $\hbar/2\pi = 55/419$; dots are for $\hbar/2\pi = 144/1097$. The quasiposition is fixed $\alpha = 0$. For the sake of comparison t and t^2 lines are shown as dashed lines.

Thus, as in the KRM, the quasiclassical Ohmic behavior appears only in a limited range of lengths, which is larger, the smaller is $\hbar$. In Fig. 3 the dependence of $\langle \ln T(\lambda)\rangle_{q_0}$ on length is shown, for a strongly incommensurate case $\hbar/2\pi = 1/(6+\rho)$, where ρ is the golden ratio, $\rho = (\sqrt{5}+1)/2$, and for a value of λ chosen at random. After a relatively small interval in which a rough agreement with the classical behavior is observed, the transmission decays exponentially. On comparing Fig. 3 with Fig. 1 we see that the Ohmic region is here narrower than for the KRM, though the ratio $D/\hbar\ell_0$, which in the KRM defines the width of this region, is roughly the same; moreover, fluctuations are definitely bigger.

In order to detect the influence of the quantum diffusion associated with the singular spectrum we have to take λ in the spectrum. A convenient strategy for locating the spectrum, and one commonly used in the study of incommensurate systems, consists in approximating the actual, incommensurate system with a periodic one. From a continuous fraction expansion one obtains a sequence of rational approximants p_n/q_n to $\hbar/2\pi = 1/(6+\rho)$. The KHM with $\hbar/2\pi = p_n/q_n$ is then a periodic approximation to the strongly incommensurate KHM with $\hbar/2\pi = 1/(6+\rho)$. The spectrum of the incommensurate KHM is approximated by the spectrum of the periodic KHM; the latter consists of bands separated by gaps, and the bands are generated as follows. Due to periodicity in q, the quasimomentum β is also conserved, besides the quasiposition α. At fixed β, α the dynamics is described by a unitary matrix of rank q_n;[11] as β is varied at fixed α, the eigenphases of this matrix sweep the bands in the spectrum of the evolution operator $\hat{U}_\alpha$, for the given α and for the given periodic approximation.

Due to absolute continuity of the spectrum, the long-time dynamics of the periodic KHM is ballistic, $(\Delta q)^2 \sim t^2$. Nevertheless, over fixed, finite scales of length and time the incommensurate dynamics will be reproduced by the periodic ones, the better the higher the chosen approximant. This is illustrated in Fig. 4, where the dependence on time of $(\Delta q)^2(t)$ is shown for the infinite KHM for two rational approximants; two lines showing the $\sim t$ and the $\sim t^2$ behavior are drawn for comparison. $(\Delta q)^2(t)$ was computed as the expectation value of q^2 over the wave function obtained at time t by iterating the KHM propagator

$$\hat{U} = e^{(ic/\hbar)\cos(\hat{q}_\alpha)} e^{(id/\hbar)\cos(\hat{p})},$$

with $\alpha = 0$ on the initial state $|0\rangle$.

Therefore, in order to analyze the scattering in a finite sample, we have chosen a suitably high approximant, and have located the spectrum by a combination of two methods: first, by computing the bands by direct diagonalization of matrices, as mentioned above; second, by analyzing the behavior of the transmission $T(\lambda)$ as a function of λ. An example of the results obtained with this procedure is shown in Fig. 5, where a scan of $T(\lambda)$ over a range of λ encompassing one of the bands obtained by diagonalization is shown.

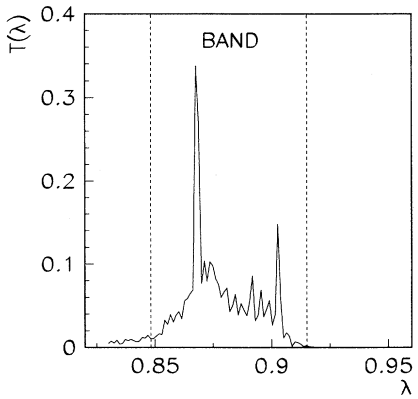

FIG. 5. Transmission coefficient as a function of quasienergy for the KHM. Here $c = d = 10$, $\hbar/2\pi = 5/38$, $L = 120$.

Statistical ensembles were generated by varying α in the interval $(0, 2\pi)$.

We have then studied the dependence of $\langle -\ln T(\lambda)\rangle_\alpha$ on length L for λ in the center of a band; the result is shown in Fig. 2. The long-time ballistic propagation (entailing a length-independent transmission) is not yet manifest in the inspected range of lengths, as confirmed by the simulation of the infinite KHM. Open circles are well fitted by the solid line of the equation

$$-\langle \ln(T)\rangle_\alpha = -1.47 + 1.14\,\ln(\hbar L),$$

giving once more a conductance inversely proportional to a power of length with an exponent close to 1, which could not be more precisely determined from our data. Thus the diffusion (with an exponent also close to 1) associated with the multifractal spectrum of the KHM results in an Ohm-like dependence of transmission on L.

However, this quantum diffusive behavior of transmission is quite different from the classical diffusive behavior, represented by the dashed line, and must therefore be considered as a purely quantum effect. A quasiclassical behavior is to be expected only in a region of very small L (hardly detectable with the parameter values used for Fig. 2), like in Fig. 1.

An obvious question is whether the difference between the classical and the quantum transmission curves could not be simply imputed to a difference between the classical and the quantum diffusion coefficients. Therefore we have computed the quantum diffusion coefficient for the case of Fig. 2 from a direct simulation of the infinite KHM; the result was in fact different from the classical coefficient ($D_q \sim D_{\rm cl}/3$), but still, on substituting this value in Eq. (3.1), we could not reproduce the quantum curve. We have therefore to conclude that the quantum transport associated with the multifractal spectrum is intimately different from classical diffusive transport.

Finally, we emphasize that on choosing different quasienergies in the spectrum different transmission curves are obtained (compare for instance open and solid circles in Fig. 2). Therefore, averaging over quasienergies (for example, over the bands) destroys the Ohmic dependence.

C. Harper model

In order to put the above results into a broader context, we now describe some results about transmission in the HM. This model does not belong in the class of kicked models discussed in Sec. II and does not possess a chaotic classical limit: Still, under appropriate conditions it exhibits a multifractal spectrum and quantum diffusion.

The Harper equation, also called almost Mathieu equation, is a 1D tight-binding equation

$$(\hat{H}_h\psi)_n = \psi_{n+1} + \psi_{n-1} + V_0\cos(Qna+\beta)\psi_n = E\psi_n, \tag{3.2}$$

where ψ_n is the wave function at site n, a is the lattice size, β is a phase, E the energy, and V_0 the potential strength. Its diffusive properties have been studied by a number of authors (for exhaustive reviews see Ref. 18 and Ref. 19).

The dynamical implications of these findings were studied in Refs. 19, 20 by solving the time-dependent Schroedinger equation

$$i\hbar\frac{\partial\psi_n}{\partial t} = (\hat{H}_h\psi)_n.$$

It was found that at the critical point $V_0 = 2$ the spreading of wave packets obeys $\mathrm{Var}(n) \sim t^\gamma$ with γ very close to 1, which means diffusive motion.

The behavior of transmission at the critical point has been investigated by many authors. Sokoloff[21] pointed out that this model has, at the critical point, for $Qa/2\pi$ a "strong" irrational number and $E = 0$ (which belongs to the spectrum), very unusual transmission properties, namely, wide fluctuations of the transmission coefficient as a function of the length (up to three orders of magnitude for variations of the length of order 1%).

At the same time it was remarked[18,22] that the transmission is an highly oscillatory function of the phase β too.

An average resistance was then introduced in Ref. 23 and used by many authors, essentially as a means for distinguishing localized states from extended ones,[19,24–28] but, to the best of our knowledge, there were no claims about its behavior as a function of length at the critical point.

We have found that, if the average over the phase β is taken, an Ohmic dependence is observed. To calculate the transmission coefficient we used the well-known transfer matrix method (see, for instance, Ref. 21). As in the previously considered models, the scattering problem is one for waves propagating on an infinite 1D lattice. Free waves have the form $\exp(ikna)$ and the corresponding dispersion law is $E = 2\cos(ka)$. The potential V_0 is different from zero only for $n = 1, \ldots, L-1$. The reflection and transmission coefficients are then found connecting the right-hand wave function $\psi_n = e^{-ikna} + re^{ikna}$ for $n \geq L$ with the left-hand wave function $\psi_n = te^{-ikna}$ for $n < 1$. The transmission coefficient is given by $T = |t|^2$.

We have fixed $E = 0$ (which belongs to the spectrum of the infinite HM because of symmetry), $Qa/2\pi = \rho = (\sqrt{5}-1)/2$, and $V_0 = 2$ (critical point). In Fig. 6 we show the average $\langle -\ln(T)\rangle$ versus $\ln(L)$. The best linear fit is the dashed line, with slope 1.02 ± 0.03 and intercept 0.5 ± 0.4. Thus we have an average "Ohmic" law, with oscillations superimposed, which are associated with the rational approximants to the golden mean. In the same Fig. 6 we also plot data related to three different rational approximants (the 7th, 9th, and 13th) to the golden mean. These data follow a continuous line up to a length $L \sim q$ (where p/q is the rational approximant); at larger lengths they saturate; i.e., transmission becomes independent of length, as expected of a pure periodic system.

As a function of β , T shows erratic fluctuations, and the distribution of $\ln(T)$ is well approximated by a log-normal distribution (for $L > 1000$); see Fig. 7. The log-normal distribution of the transmission coefficient is a nontrivial occurrence, because the spectrum is singular

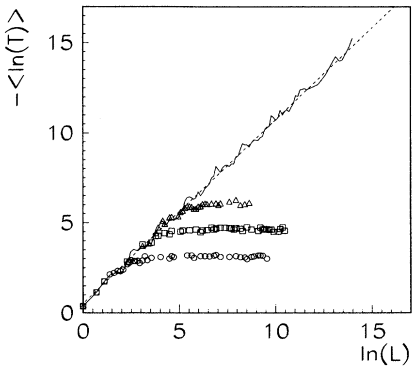

FIG. 6. Transmission versus length for the HM. Here $E = 0$, $V_0 = 2$, $Qa/2\pi = \rho$, ρ the golden mean. Each point is obtained by averaging over an ensemble of 10^3 random phases β. Circles, squares, and triangles are, respectively, for the 7th, 9th, and 13th approximants to the golden mean. The dashed line is the best fit line with slope 1.02(3).

continuous and not pure point (the localized phase is known to exhibit a lognormal transmission distribution).

Averaging over β the logarithm of T rather than T itself was quite effective in significantly reducing fluctuations. Huge fluctuations of $\langle T\rangle_\beta$ are indeed observed when the sample length is equal to a multiple of the denominator of the rational approximants to $Qa/2\pi$; see, for instance, the solid line in Fig. 8. This effect is particularly evident at small length, where only a few "resonances" are present.

On checking the stability of these results against changes of the energy E and of the modulation Qa, two relevant aspects emerge. On the one hand, no significant changes appear if the energy is changed inside the spectrum, but far from the band edges (this was done as in Sec. III B). On the other hand, a different irrational modulation (quadratic or transcendental numbers) yields a different power law, as can be inferred from Table I. For brevity we call such a dependence a "generalized Ohm's law" and the corresponding exponent an "Ohmic exponent" (OE).

The OE in the third column of Table I is obtained from the best linear fit of $\langle -\ln(T)\rangle_\beta$ vs $\ln(L)$; the error in the last digit is indicated in brackets, and the continuous fraction expansion is given in the second column.

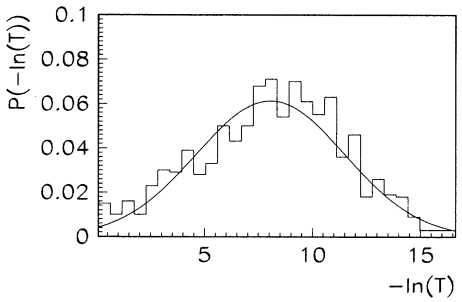

FIG. 7. Distribution of the transmission coefficient for the HM, at fixed length $L = 1000$, by varying randomly β in $[0, \pi]$, for $E = 0$, $V_0 = 2$, $Qa/2\pi = \rho$. The solid line is the Gaussian obtained from the standard best fitting procedure.

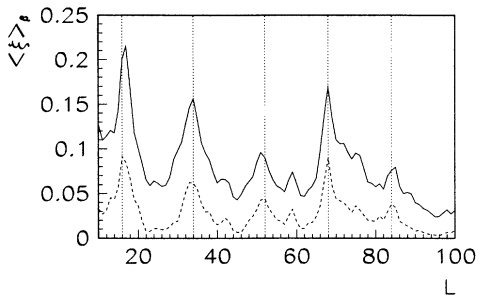

FIG. 8. β-averaged transmission coefficient (solid line $\xi = T$) and its variance [dashed line $\xi = \mathrm{Var}(T)$] as a function of the length L for the same data as Fig. 7. As vertical lines are shown multiples of the rational approximants to ρ: $13, 21, 34, 55, \ldots$. Averaged values were computed by taking 5000 random β in the interval $[0, \pi]$.

The degree of irrationality of $Qa/2\pi$, rather than its absolute value, appears to determine the exponent of the algebraic decay of the transmission. In fact two different numbers only differing in the first terms of their continued fraction expansion (the golden mean and $[100, 1, 1, 1, \ldots]$) produce practically the same exponent. The fact that in Table I the exponent 1 (or very close to 1) occurs only for these two numbers raises the question of whether such an exponent is connected to a noble irrational modulation. Different choices of Qa, even in the class of the irrational algebraic numbers, produces a different OE.

The last point is crucial, because, as reported in Ref. 29, the dynamical exponent ruling the spreading in time of wave packets in the infinite Harper model is practically independent of Qa (provided it is sufficiently irrational), and so appears to be the scaling properties of the spectrum.[30]

This means that the OE is not directly connected with the spectral properties, and must therefore be determined by the structure of the eigenfunctions. Scaling properties for the latter have been found,[27] which, however, do not hold for generic irrational (e.g., transcendental) modulation, and cannot therefore by themselves explain the generalized Ohm's law, which is observed even for such numbers (bottom of Table I).

TABLE I. Generalized Ohm's exponent for various irrational modulations.

$Qa/2\pi$	Expansion	OE
$(\sqrt{5}-1)/2$	$[1,1,1,1,\ldots]$	1.02(3)
$(197-\sqrt{5})/19402$	$[100,1,1,1,\ldots]$	1.00(5)
$\sqrt{2}-1$	$[2,2,2,2,\ldots]$	1.35(4)
$\sqrt{3}-1$	$[1,2,1,2,\ldots]$	1.15(8)
$(\sqrt{3}-1)/2$	$[2,1,2,1,\ldots]$	1.15(3)
$(\sqrt{37}-4)/3$	$[1,2,3,1,2,3,\ldots]$	1.28(4)
$e-2$	$[1,2,1,1,4,\ldots]$	0.75(3)
$\pi-3$	$[7,15,1,292,1,\ldots]$	0.38(3)

IV. TRANSMISSION FLUCTUATIONS

In the previous sections we have studied the implications that a diffusive spread of wave packets, whether of a quasiclassical origin or due to a fractal spectrum, has on the average transmission. In this section we shall instead analyze the fluctuations of the transmission.

In the theory of transmission through disordered solids, the quantum diffusive regime is characterized by universal conductance fluctuations (UCF's), i.e., by transmission fluctuations of scale-independent magnitude.[31–48] On defining the dimensionless conductance as $G = \chi T$, where χ is the number of scattering channels, it was found that

$$\mathrm{Var}(G) \approx \frac{2}{15}$$

for a time-reversal-invariant transmission process[34,31,33,48] through a quasi-one-dimensional sample of length L, with $\ell_0 \ll L \ll \ell$. Such universal fluctuations are considered a distinctive mark of a proper quantum diffusive regime, besides the validity of Ohm's law (apart from weak-localization corrections).

As mentioned in Sec. III A, the KRM exhibits UCF's.[5,6] In Figs. 9,10 we present results for the other two models examined in this paper which do not share this property. Data for the KHM (Fig. 9) are rather ambiguous. In fact, even if the points are distributed along the line 2/15 (their average value is 0.12), they appear at the same time slowly decreasing with length. This behavior is especially clear with the HM (Fig. 10), where a power-law dependence on length is found: $\mathrm{Var}(T) \sim L^{-\delta}$ with $\delta = 0.38 \pm 0.04$ (in this case conductance and transmission coefficient are the same since only the "in" and "out" scattering channels are active).

One more feature preventing fluctuations from being length independent is the presence of sharp variations of $\mathrm{Var}(T)$ as a function of the sample length L, when L is some multiple of a denominator occurring in rational approximants of $Qa/2\pi$. This behavior does not appear to be due to insufficient statistics, and is shown by a dashed line in Fig. 8. Therefore, although the range of lengths inspected in Figs. 9 and 10 is "Ohmic" for transmission, transmission fluctuations are not universal, because $\mathrm{Var}(T)$ is length dependent. UCF's appear then to be typical of quasiclassical diffusion.

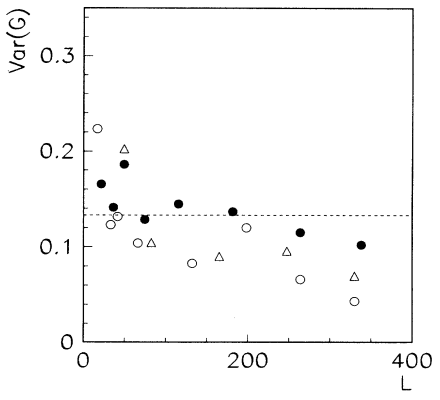

FIG. 9. $\mathrm{Var}(G)$ versus the length for the KHM. Open and solid circles are obtained by fixing two different quasienergies and varying the quasiposition over 100 samples; triangles are obtained by varying the quasienergy over 100 samples and fixing the quasiposition $\alpha = 0$. The horizontal dashed line is the theoretical value 2/15.

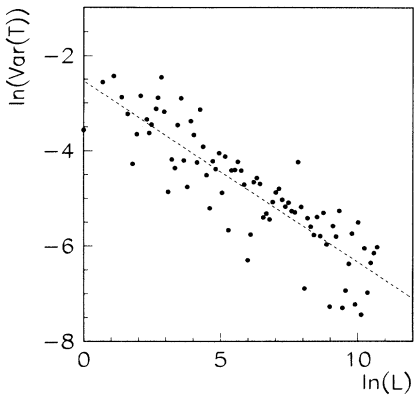

FIG. 10. $\ln[\mathrm{Var}(T)]$ versus the logarithm of the length for the HM. Here $E = 0$, $V_0 = 2$, $Qa/2\pi = \rho$. Each point is obtained by averaging over 10^3 different samples. The dashed line is the best fit line with slope $\delta = -0.38 \pm 0.04$.

Finally we remark that in the Harper model the transmission remains a non-self-averaging quantity,[48] since $\mathrm{Var}(T)/\langle T\rangle^2$ diverges algebraically with L when $L \to \infty$.

V. CONCLUSIONS

The Ohmic dependence of transmission on the sample length is a typical feature of classical one-dimensional diffusive transport, which can be observed in strictly deterministic classical systems in the presence of a chaotic dynamics. On the other hand, one-dimensional chaotic diffusion is typically suppressed, in the long run, by quantization, so that an Ohmic behavior can be quantally observed only on length scales which are small in comparison to the quantum localization length. In some cases, however, localization effects leave room for an unbounded pseudodiffusive spread of wave packets, connected with a fractal structure of the energy (or quasienergy) spectrum. On analyzing the transmission properties associated with such a "fractal" pseudodiffusion, which is observed in a model endowed with a chaotic classical limit, we have found evidence that this kind of quantum diffusion is a purely quantum effect, as unrelated to quasiclassical chaotic diffusion as is quantum localization itself. On comparing the behavior of the kicked Harper model, which exhibits both types of diffusion, with the kicked rotator model on the one hand, and with the Harper model on the other, it becomes apparent that the proper Ohmic regime is still restricted to a range of "small" sample lengths, in which the singular continuous nature of the spectrum is still unresolved (as was the singular pointlike spectrum of the kicked rotator model),

and the quantum motion is essentially a quasiclassical diffusion. Beyond that, the purely quantum pseudodiffusion alone is at work, leading to a substantially different type of transmission, which is still power-law dependent on the length, but with an exponent which depends on the arithmetic nature of the Planck's constant, according to as-yet unknown rules, and cannot therefore be meaningfully carried to the classical limit. In addition, the statistics of transmission fluctuations are quite different from the quasiclassical case; in particular, their magnitude is not scale independent, as it should be in a proper metallic regime. In the language of the theory of quantum chaotic scattering, the crucial aspects of the Ericson regime of strongly overlapped scattering resonances appear to be lost as soon as the continuous (singular) nature of the spectrum comes into play.

ACKNOWLEDGMENTS

We thank Roberto Artuso for help in numerical computations and Dima Shepelyansky for useful discussions.

[1] A.J. Lichtenberg and M.A. Lieberman, *Regular and Stochastic Motion*, Applied Mathematics Series Vol. 38 (Springer, New York, 1983).
[2] B.V. Chirikov, Phys. Rep. **52**, 263 (1979).
[3] A.B. Rechester, M.N. Rosenbluth, and R.B. White, Phys. Rev. A **23**, 2264 (1981).
[4] F. Izrailev, Phys. Rep. **196**, 207 (1990).
[5] F. Borgonovi and I. Guarneri, J. Phys. A **25**, 3239 (1992); in *Quantum Chaos—Quantum Measurement*, Proceedings of the NATO school on Quantum Chaos, edited by P. Cvitanovic *et al.* (Kluwer, Dordrecht, 1992), pp. 73–80.
[6] F. Borgonovi, I. Guarneri, and L. Rebuzzini, Phys. Rev. Lett. **72**, 1463 (1994).
[7] P. Leboeuf, J. Kurchan, M. Feingold, and D.P. Arovas, Phys. Rev. Lett. **65**, 3076 (1990).
[8] R.A. Pasmanter, Phys. Rev. A **42**, 3622 (1990).
[9] R. Lima and D. Shepelyansky, Phys. Rev. Lett. **67**, 1377 (1991).
[10] D. Shepelyansky, in *Quantum Chaos—Theory and Experiments*, edited by P. Cvitanovic, I.C. Percival, and A. Wirzba (Kluwer, Dordrecht, 1992).
[11] I. Guarneri and F. Borgonovi, J. Phys. A **26**, 119 (1993).
[12] R. Artuso, F. Borgonovi, I. Guarneri, L. Rebuzzini, and G. Casati, Phys. Rev. Lett. **69**, 3302 (1992).
[13] T. Geisel, R. Ketzmerick, and G. Petschel, Phys. Rev. Lett. **67**, 3635 (1991).
[14] R. Ketzmerick, G. Petschel, and T. Geisel, Phys. Rev. Lett. **69**, 695 (1992).
[15] R. Artuso, F. Borgonovi, G. Casati, I. Guarneri, and L. Rebuzzini, Int. J. Mod. Phys. B **8**, 207 (1994).
[16] I. Guarneri, Europhys. Lett. **10**, 95 (1989); **21**, 729 (1993).
[17] I. Guarneri and G. Mantica, Ann. Inst. H. Poincaré **61**, 369 (1994).
[18] J.B. Sokoloff, Phys. Rep. **126**, 189 (1985).
[19] H. Hiramoto and M. Kohmoto, Int. J. Mod. Phys. B **6**, 281 (1992).
[20] T. Geisel, R. Ketzmerick, and G. Petschel, Phys. Rev. Lett. **66**, 1651 (1991).
[21] J.B. Sokoloff, J. Phys. C **17**, 1703 (1984).
[22] S. Ostlund and R. Pandit, Phys. Rev. B **29**, 1394 (1984).
[23] M. Rubinstein and M.Ya. Azbel, Phys. Rev. B **27**, 6484 (1984).
[24] T.C. Halsey, M.H. Jensen, L.P. Kadanoff, I. Procaccia, and B.I. Shraiman, Phys. Rev. A **33**, 1141 (1986).
[25] You-Yan Liu, R. Riklund, and K.A. Chao, Phys. Rev. B **32**, 8387 (1985); **34**, 5247 (1986); You-Yan Liu, *ibid.* **37**, 9694 (1988).
[26] B. Sutherland and M. Kohmoto, Phys. Rev. B **36**, 5877 (1987).
[27] D. Dominguez, C. Wiecko, and J.V. Jose, Phys. Rev. B **45**, 13919 (1992).
[28] A.K. Gupta and A.K. Sen, J. Phys. (France), I **2**, 2039 (1992).
[29] H. Hiramoto and S. Abe, J. Phys. Soc. Jpn. **57**, 230 (1988); **57**, 1365 (1988).
[30] C. Tang and M. Kohmoto, Phys. Rev. B **34**, 2041 (1986).
[31] Y. Imry, Europhys. Lett. **1**, 249 (1986).
[32] J.L. Pichard, J. Phys. C **19**, 1519 (1986).
[33] J.L. Pichard, in *Quantum Coherence in Mesoscopic Systems*, edited by B. Kramer, Vol. XX of NATO Advanced Study Institute, Series B: Physics (Plenum, New York, 1990).
[34] P.A. Mello, Phys. Rev. Lett. **60**, 1089 (1988).
[35] E. Abrahams, P.W. Anderson, D.C. Licciardello, and T.V. Ramakrishnan, Phys. Rev. Lett. **42**, 637 (1979).
[36] B.S. Andereck and E. Abrahams, J. Phys. C **13**, L383 (1980).
[37] P.W. Anderson, D.J. Thouless, E. Abrahams, and D.S. Fisher, Phys. Rev. B **22**, 3519 (1980).
[38] A.D. Stone, J.D. Joannopoulos, and D.J. Chadi, Phys. Rev. B **24**, 5583 (1981).
[39] M. Buttiker, Y. Imry, R. Landauer, and S. Pinhas, Phys. Rev. B **31**, 6207 (1985).
[40] P.A. Lee and A.D. Stone, Phys. Rev. Lett. **55**, 1622 (1985).
[41] S. Washburn and R.A. Webb, Adv. in Phys. **35**, 375 (1986).
[42] M. Kaveh, M. Rosenbluth, I. Edrei, and I. Freund, Phys. Rev. Lett. **57**, 2049 (1986).
[43] S.N. Evangelou, in *Disordered Systems and New Materials*, edited by N. Kirov, M. Borissov, and A. Vavrek (World Scientific, Singapore, 1989), p. 783.
[44] S. Iida, H.A. Weidenmuller, and J.A. Zuk, Phys. Rev. Lett. **64**, 583 (1990).
[45] J.L. D'Amato and H.M. Pastawski, Phys. Rev. B **41**, 7411 (1990).
[46] K.A. Muttalib, Phys. Rev. Lett. **65**, 745 (1990).
[47] S. Gangopadhyay and A.K. Sen, Phys. Rev. B **46**, 4020 (1992).
[48] P.A. Lee, A.D. Stone, and H. Fukuyama, Phys. Rev. B **35**, 1039 (1987).